Resting-state network topology and planning ability in healthy adults

Authors

Chris Vriend, PhD[1,2], Margot J. Wagenmakers, Msc[1], Odile A. van den Heuvel, MD PhD[1,2], Ysbrand D. van der Werf, PhD[1]

Affiliations

1 Amsterdam UMC, Vrije Universiteit Amsterdam, Department of Anatomy & Neurosciences, Amsterdam Neuroscience, De Boelelaan 1117, Amsterdam, Netherlands;

2 Amsterdam UMC, Vrije Universiteit Amsterdam, Department of Psychiatry, Amsterdam Neuroscience, De Boelelaan 1117, Amsterdam, Netherlands.

[#] Corresponding author:

C. Vriend, PhD, Amsterdam UMC | location VUmc, Department of Anatomy and Neuroscience, p/a sec. ANW O|2, PO Box 7007, 1007MB BT, Amsterdam, the Netherlands. E-mail: c.vriend@amsterdamumc.nl, telephone: +31 20 4449635, fax: +31 20 4448054

Running title: Resting-state network topology and planning

Word count

Character count title: 69

Word count manuscript, excluding references and tables/figures: 3676

Word count abstract: 250

References = 67; # Tables = 2; # Figures = 4

Abstract

Functional magnetic resonance imaging (fMRI) studies have been used extensively to investigate the brain areas that are recruited during the Tower of London (ToL) task. Nevertheless, little research has been devoted to study the neural correlates of the ToL task using a network approach. Here we investigated the association between functional connectivity and network topology during resting-state fMRI and ToL task performance, that was performed outside the scanner. Sixty-two (62) healthy subjects (21-74 years) underwent eyes-closed rsfMRI and performed the task on a laptop. We studied global (whole-brain) and within subnetwork resting-state topology as well as functional connectivity between subnetworks, with a focus on the default-mode, fronto-parietal and dorsal and ventral attention networks. Efficiency and clustering coefficient were calculated to measure network integration and segregation, respectively, at both the global and subnetwork level. Our main finding was that higher global efficiency was associated with slower performance ($\beta = .22$, $P_{bca} = .04$) and this association seemed mainly driven by inter-individual differences in default-mode network connectivity. The reported results were independent from age, sex, education-level and motion. Although this finding is contrary to earlier findings on general cognition, we tentatively hypothesize that the reported association may indicate that individuals with a more integrated brain during the resting-state are less able to further increase network efficiency when transitioning from a rest to task state, leading to slower responses. This study also adds to a growing body of literature supporting a central role for the default-mode network in individual differences in cognitive performance.

Keywords: functional connectivity, resting-state, network analysis, planning, cognition, default-mode network.

Introduction

Executive functions are a set of mental processes that enable us to plan, focus attention, remember instructions and handle several tasks at once (Diamond, 2013). Functional magnetic resonance imaging (fMRI) studies have shown that these functions are associated with functional connectivity (FC) of certain resting-state networks (RSN) (Funahashi & Andreau, 2013; Nowrangi, Lyketsos, Rao, & Munro, 2014; Rabinovici, Stephens, & Possin, 2015). Various RSN have been shown to be involved in executive functions, including the default mode network (DMN) which is active during rest and deactivates during task performance (Anticevic et al., 2012; Buckner, Andrews-Hanna, & Schacter, 2008; Mak et al., 2017). Other relevant RSN for cognition are the frontoparietal network (FPN) (M. W. Cole, Repovs, & Anticevic, 2014; M. W. Cole, Yarkoni, Repovs, Anticevic, & Braver, 2012) and the dorsal and ventral attention networks (DAN and VAN, respectively) (Fortenbaugh, Rothlein, McGlinchey, DeGutis, & Esterman, 2018). Although the utility of RSN in cognitive neuroscience and understanding of the neural correlates of cognition has been debated (Campbell & Schacter, 2017; Davis, Stanley, Moscovitch, & Cabeza, 2017; Iordan & Reuter-Lorenz, 2017), resting-state FC patterns show good correspondence with task-based FC patterns (Krienen, Yeo, & Buckner, 2014), are fundamentally stable (Gratton et al., 2018) and may act as an intrinsic network architecture that shapes FC when evoked by a cognitive task (M. W. Cole, Bassett, Power, Braver, & Petersen, 2014; Ito et al., 2017).

The architecture or topology of the brain can be studied using graph analysis, where the brain is simplified to a graph of nodes (i.e., different brain regions) and edges (i.e., connections between brain regions) (Bullmore & Sporns, 2009; Wang, Zuo, & He, 2010). Different properties of the brain network can be calculated using this graph. For example, efficiency and clustering describe the ability of a network to integrate and segregate information, respectively (Cohen & D'Esposito, 2016; Lord, Stevner, Deco, & Kringelbach, 2017). The brain balances its ability to integrate and easily transmit information throughout the network, and to segregate information processing in clusters of highly interconnected (specialized) neighboring nodes (Bullmore & Sporns, 2009). This ability of the brain for

integration and segregation is vital for cognitive processes (Cohen & D'Esposito, 2016) and higher intelligence has been associated with a more efficient network topology (Langer et al., 2012; M. P. van den Heuvel, Stam, Kahn, & Hulshoff Pol, 2009). Conversely, dementia and cognitive impairments in the light of brain disorders generally show dysfunction in the brain's ability to functionally integrate and segregate information (Dai et al., 2019; Lopes et al., 2017; Rocca et al., 2016). Nevertheless, studies on the associations between network topology and inter-individual differences in cognitive functions in healthy subjects are relatively scarce, e.g. (Cohen & D'Esposito, 2016; Sheffield et al., 2017), and to the best of our knowledge, no study has yet focused on the association between network topology and planning capacity. Planning is the ability to think ahead in order to achieve a goal via a series of intermediate steps (Owen, 1997) and is a vital function in daily life that we here operationalize in the form of the Tower of London (ToL) task. In this study, we investigated the association between RSN topology and planning performance, using a graph-based approach. Based on prior research (Langer et al., 2012; Sheffield et al., 2017; M. P. van den Heuvel et al., 2009), we hypothesized a positive relationship between network topology measured during resting-state and cognitive planning ability, measured using the ToL task performed outside of the scanner.

Methods

Subjects and measurements

Data of healthy adult controls from two previous case-control studies (de Wit et al., 2012; Gerrits et al., 2015) were pooled for the current study. Exclusion criteria for all healthy subjects were the use of psychoactive medication, current or past psychiatric diagnosis, a history of a major physical or neurological illness, MRI contraindications or a history of alcohol abuse. Further exclusion criteria for the current study were: no available data on the ToL task, extreme behavioral scores (≥ 2 SD from the mean), a time-interval of more than 21 days between resting-state fMRI (rs-fMRI) and performing the ToL task, or pathological incidental findings on the structural MRI scan. Written informed consent was provided by all participants according to the Declaration of Helsinki and the studies were approved by the Medical Ethical Committee of the VU University Medical Centre (Amsterdam, The Netherlands).

The participants performed a computerized version of the ToL task as a measure of planning (Phillips, Wynn, McPherson, & Gilhooly, 2001; Shallice, 1982). Details of the ToL task are provided in the study by (O. A. van den Heuvel et al., 2003) . In short, the participants saw two configurations ("begin" and "goal" position) of three colored beads on vertical posts of different heights. The purpose of the task is to determine the minimum number of moves (1, 2, 3, 4, or 5) needed to match the configuration of the goal position. Participants responded via the matching keyboard-button. The first post can hold all three beads, the second two, and the third post one. Only one bead can be moved at a time and only if there is no other bead on top of it. Prior to the experiment, participants were provided verbal and written explanation and performed a practice run. Performance on the ToL task was indicated by the mean accuracy and mean reaction time across all five difficulty levels (Kaller et al., 2016). Intelligence scores were approximated by the Dutch Adult Reading test (NLV; (Schmand, Bakker, Saan, & Louman, 1991). We scored education level according to the Dutch Verhage scale (Verhage, 1964) that ranges from 1 - *primary school not finished*, to 7 – *university or higher.* Handedness was assessed using the Edinburgh Handedness Inventory (Oldfield, 1971).

MR Image acquisition

MR images were acquired at Amsterdam UMC, location VUmc (Amsterdam, The Netherlands) on a GE Signa HDxt 3 Tesla MRI scanner (General Electric, Milwaukee, WI) with an eight channel head coil. The participant's head was immobilized using foam pads to reduce motion artifacts. Participants were told to lie still, keep their eyes closed and not fall asleep during the acquisition of the rs-fMRI scan (duration: 5.9 min). T2*-weighted echo-planar (EPI) images were acquired with TR = 1.8 sec, TE = 30 ms, 64x64 matrix, field of view = 24 cm and flip angle = 80° and 40 ascending slices per volume (3.75 x 3.75 mm in plane resolution; slice thickness = 2.8 mm; interslice gap = 0.2 mm). Structural scanning encompassed a sagittal three-dimensional gradient-echo T1-weighted sequence (256 x 256 matrix; voxel size = 1 x 0.977 x 0.977 mm; 172 slices).

Image (pre)processing

RS-fMRI and T1-weighted images were preprocessed with FMRIB's Software Library version 5.0.10 (FSL; (Smith et al., 2004)). The first four volumes were discarded to reach steady-state magnetization. Non-brain tissue was removed using BET and the structural image was segmented into gray (GM), white matter (WM) and cerebrospinal fluid (CSF) using FAST. Functional images were re-aligned using McFLIRT and the resulting six rigid-body parameters were used to calculate the motion parameters. Functional images were spatially smoothed with a 5 mm full width at half maximum (FWHM) kernel. Subjects with significant motion during scanning, defined as a mean relative root mean squared displacement (RMS) > 0.2 mm, or > 20 volumes with frame-wise relative RMS displacement > 0.25 mm, were excluded (Ciric et al., 2017). Because rs-fMRI is exceptionally sensitive to motion artefacts (Power, Schlaggar, & Petersen, 2015), we additionally performed ICA-AROMA (Pruim et al. 2015). ICA-AROMA is a single-subject denoising strategy based on independent component analysis (ICA) that automatically identifies motion-related components in the functional data based on their high-frequency content, correlation with the motion parameters and edge and CSF fraction and removes

their variance from the data (Pruim et al., 2015). ICA-AROMA has been shown to provide a good trade-off between reducing noise and preserving BOLD signal (Ciric et al., 2017; Parkes, Fulcher, Yucel, & Fornito, 2018; Pruim et al., 2015). After ICA-AROMA, additional nuisance regression was performed by removing signal from the WM and CSF and functional images were high-pass filtered (100 seconds cut-off).

The functional scan was non-linearly registered to the anatomical T1-scans. The anatomical image was parcellated into 225 nodes; 210 cortical nodes were defined based on the Brainnetome Atlas (Fan et al., 2016), 14 subcortical nodes were individually segmented using FSL FIRST (Patenaude, Smith, Kennedy, & Jenkinson, 2011) and one cerebellar node was defined based on the FSL's cerebellar atlas (Diedrichsen, Balsters, Flavell, Cussans, & Ramnani, 2009). EPI distortions during fMRI can lead to signal drop-out. To account for signal dropout near air/tissue boundaries during scanning, we applied a mask to the functional scan to exclude voxels with signal intensities in the lowest quartile of the robust range (Meijer et al., 2017). Nodes were discarded if they comprised less than four signal-containing voxels. This rendered a total of 194 common brain regions across all subjects. Time-series were extracted from each node. The cortical nodes were subdivided into four RSN: the DMN, FPN, DAN and VAN based on the functional subdivision by Yeo et al. (2011).

Functional connectivity matrices

To measure FC and construct connectivity matrices we applied wavelet coherence on the time-series of each possible pair of the 194 brain regions within the frequency range 0.06 and 0.12 Hz (Chang & Glover, 2010). Wavelet coherence has several advantages over Pearson's correlations, including denoising properties and robustness to outliers (Achard, Salvador, Whitcher, Suckling, & Bullmore, 2006; Fadili & Bullmore, 2004; Gu et al., 2017). The 0.06-0.12Hz frequency range was chosen because it has been suggested to be a reliable and robust range that is associated with cognitive performance (Bassett et al., 2013; Zhang, Telesford, Giusti, Lim, & Bassett, 2016). We applied wavelet coherence to

the entire rs-fMRI scan to calculate the network measures (see below). An overview of the (pre)processing pipeline is provided in Figure 1.

Network measures

At the global level we calculated global efficiency and global clustering coefficient (Gcc). Global efficiency is the inverse of the average path length (i.e. the maximum connectivity between each pair of nodes), with high efficiency meaning that information can rapidly travel through the whole network (Latora & Marchiori, 2001). Gcc is equivalent to the proportion of the actual number of edges between the nearest neighbors of a node to all possible edges and signifies the tendency of the whole network to segregate into locally interconnected triplets that function as a specialized subunit (Rubinov & Sporns, 2010). At the subnetwork level, we calculated efficiency and clustering coefficient for each of the four RSNs (DMN, FPN, DAN and VAN). In addition, we determined the mean FC *between* each of the four RSNs (resulting in six between-network mean FC values).

Data analysis

Statistical analyses were performed using SPSS version 25 (IBM Corp, Armonk, NY, USA). We describe demographical characteristics and performance on the ToL task using means and standard deviations, unless indicated otherwise. Pearson's (r) or Spearman's rho (r_s) correlations were performed between demographic and performance measures, depending on the distribution. We performed bootstrapped hierarchal multiple regression analysis to investigate the association between network measures (predictors) and accuracy and reaction time on the ToL task (outcome measures). Because age was correlated with performance, age was entered in the first block of all models. The network measure of interest and mean RMS displacement, as a measure for motion, were entered in the second and third block, respectively. As a sensitivity analysis, we entered sex or education level to the fourth block of

the model. The regression models were bootstrapped using 2000 iterations and bias corrected and we report accelerated (BCa) confidence intervals and P-values (P_{bca}) for a more robust estimate of the association that is less reliant on the distribution of the variable. All assumptions of multiple regression analyses, including homoscedasticity of residuals, were assessed and met. We performed separate analyses for the network measures on the global level and on the subnetwork level. On the subnetwork level, type I errors due to multiple comparisons were minimized using the False Discovery Rate (FDR, q<.05 (Benjamini & Hochberg, 1995)). Statistical significance was set to $p < 0.05$ for all analyses.

Results

Sample characteristics and behavioral results

Of the 69 participants with an available ToL task and rs-fMRI data, seven had to be excluded (see figure 2), which resulted in a total sample size of 62 participants, aged between 21 and 74 years old (M_{age} = 48.1 ± 13.9, 33 males). The time between performing the ToL task and the rs-fMRI was on average 6.2 ± 4.6 [range: 0-21] days. See Table 1 for the sample characteristics. Age showed a positive correlation with reaction time (r = .498, p < .001) but only a trend-level negative correlation with accuracy (r = -.243, p = .057) indicating that older participants tended to respond slower and slightly less accurately. The average motion during rs-fMRI (expressed as mean relative RMS framewise displacement) was 0.068 ± 0.029 [range: 0.027-0.17] and was positively correlated with age (r_s = .34, p = .007) but not performance on the ToL (reaction time: r_s = .06, p = .66; accuracy: r_s = -.18, p = .12).

Global topology

Global efficiency (β = .22, P_{bca} = .04) but not Gcc (β = -.09, P_{bca} = .57) was positively associated with reaction time above and beyond the effects of age (see Table 2). There were no significant

associations with accuracy. Adding sex or education level as a nuisance covariate to the model had no effect on these results.

Subnetwork topology

Both efficiency and clustering of the DMN (efficiency: β = .25, P_{bca} = .018; clustering: β = .23, P_{bca} = .039) but not the other subnetworks (see supplemental Table 1) were positively related to reaction time. These associations did not, however, survive the multiple comparison correction (DMN efficiency P_{fdr} = 0.072; DMN clustering: P_{fdr} = 0.077). Adding sex or education level as additional nuisance covariate to the model had no effect on the results. Consistent with the results on the global level, there were no significant associations with accuracy of task performance (Supplemental Table 2).

Between-subnetwork connectivity

FC between the DMN and FPN (β = .23, P_{bca} = .04), the DAN (β = .21 P_{bca} = .04) and the VAN (β = .20, P_{bca} = .04) were all positively associated with reaction time. These associations did not survive the FDR correction for multiple comparisons (all P_{fdr} = .09; supplemental Table 3 and 4).

Post-hoc analyses

Because of possible floor/ceiling effects during the less demanding 1, 2 and 3 step trials of the ToL task, we re-ran the regression models using only the mean accuracy rates and reaction times during ToL steps 4 and 5. These post-hoc analyses showed that at the global level reaction time – but not accuracy – was still associated with global efficiency (β = .27, P_{bca} = .04), not Gcc (β = -.09, P_{bca} = .59). At the subnetwork level, efficiency of the DMN (β = .41, P_{fdr} = .001) and FPN (β = .32, P_{fdr} = .045), clustering of the DMN (β = .33, P_{fdr} = .05) and FC between the DMN and FPN (β = .38, P_{fdr} = .02) were all positively associated with reaction time, after FDR correction for multiple comparisons.

Discussion

In this study in 62 healthy adults with a wide age range we investigated the association between network topology during a rs-fMRI session and cognitive planning ability during a ToL task that was performed outside the scanner. We observed that global (whole-brain) efficiency was associated with reduced planning speed and that this effect was mainly driven by the FC of the DMN. The results were independent from inter-individual differences in age, gender, education level and motion during rs-fMRI. Post-hoc analyses showed that our results were strongest when focusing on the higher task load trials of the ToL task (four and five step trials).

Global efficiency provides a measure of how well-integrated a network is and how easily information can travel from one node to another on the other side of the network, while the clustering coefficient is a measure of how well-connected nodes are locally into segregated triangles of neighboring nodes. Both measures are often used to describe the characteristics of a network and abnormalities in these network measures are commonly observed in the structural and functional networks of patients with a brain disorder (Bullmore & Sporns, 2012; Griffa, Baumann, Thiran, & Hagmann, 2013; Lord et al., 2017; Worbe, 2015). Here we observed that subjects with a higher global efficiency show slower planning performance on the ToL task. This finding is at odds with our hypothesis and previous studies that observed that higher global efficiency is associated with higher global intelligence (Sheffield et al., 2017; M. P. van den Heuvel et al., 2009) and performance on working memory tasks (Cohen & D'Esposito, 2016; Sheffield et al., 2015). One other study has also previously found that a higher global efficiency was associated with worse performance on a working memory task, but only in older adults and only when focusing on task-based FC (Stanley et al., 2015). This is the first study, however, to investigate planning ability. One possible, albeit less plausible, explanation might therefore be that planning requires a different whole-brain network organization than working memory tasks or general intelligence. Alternatively, the higher global efficiency in individuals with slower performance on the ToL task may also point towards a more random network (Ajilore, Lamar, & Kumar, 2014). As there

was no association between ToL task speed and lower global clustering (a characteristic feature of random networks), this explanation is also less viable.

Studies have shown that, although the resting-state provides a core and intrinsic network architecture that highly overlaps with the network topology of task-states (D. M. Cole, Smith, & Beckmann, 2010; Krienen et al., 2014), significant reorganization does take place during the execution of tasks, and the magnitude and spatial redistribution depends on the task and its load (Cohen & D'Esposito, 2016; Davison et al., 2015). Furthermore, the ease with which a network can reconfigure from rest to task-states correlates with task performance and general cognition (Bassett et al., 2011; Braun et al., 2015; Hearne, Cocchi, Zalesky, & Mattingley, 2017; Telesford et al., 2016). Transitions of rest to (demanding) task-states have generally been associated with an increase in global efficiency, signifying a better integrated network (Cohen & D'Esposito, 2016; Hearne et al., 2017; Shine et al., 2016; see Shine & Poldrack, 2018 for a review). This increase in network integration is, however, not unconstrained, as a fully integrated functional network would lead to epileptic seizures and violates the principles of cost-efficiency (Bullmore & Sporns, 2012; Shine & Poldrack, 2018). Assuming that in our subjects network integration would similarly increase from the resting-state to task-state, i.e. execution of the ToL task, it is conceivable that global efficiency could not increase sufficiently in those subjects with an already highly integrated network during the resting-state to meet task demands, leading to a slower behavioral response. This concept is schematically depicted in Figure 4. Although this hypothesis receives indirect support from multiple previous studies on dynamic network reconfigurations (Shine & Poldrack, 2018), we unfortunately did not acquire fMRI scans during execution of the ToL task and therefore this explanation currently remains speculative. Because the slower responses were not associated with lower accuracy (r_s = -.19 , P = .13) and we did not observe an association between network topology and accuracy, our results may not be specific for planning performance but may also be related to an overall slower information processing speed. Why we did not find an association with task accuracy is currently unclear.

At the subnetwork level, we showed that our global results were mainly driven by inter-individual differences in FC of the DMN; both the topology of the DMN and FC between the DMN and the other RSNs (mainly the FPN) were associated with slower task performance. Because closer inspection showed that efficiency and clustering of the DMN were highly correlated (r = 0.84), the observed positive associations should instead be interpreted as an association between slower performance and increased *within* DMN FC. Indeed, when looking at total FC within the DMN, we observed a positive association (β = .25, P_{bca} = .02) with ToL reaction time. It is generally accepted that activity within the DMN is high when a subject is not engaged in any specific task and its activity is suppressed when external stimuli demand cognitive engagement (Anticevic et al., 2012). Heightened DMN activity and higher FC between the DMN and other RSNs are also commonly associated with reduced cognitive performance in brain disorder-related deficits (Anticevic et al., 2012; Esposito et al., 2018; Putcha, Ross, Cronin-Golomb, Janes, & Stern, 2016). Our associations between slower ToL performance and increased within DMN FC and increased connectivity between the DMN and the other RSNs is therefore in line with these findings and adds to the growing body of literature that shows that inter-individual differences in FC of the DMN is associated with cognitive performance, even in normally functioning healthy subjects. It must be noted that these associations did not survive the multiple comparison correction, although the reported associations between performance speed at higher task load and within DMN FC and FC between DMN and FPN in our post-hoc analysis did pass the FDR correction.

A limitation of this study is that we exclusively looked at resting-state FC to predict performance on the ToL and not –at task-based FC, i.e. during execution of the ToL itself. This would have allowed us to look directly at the network characteristics associated with performance and to test our hypothesis of reduced ability to network integration when transitioning from rest to task. A strength of this study is that we retrospectively recruited a relatively large number of healthy subjects and used stringent control for (micro)motion by excluding subjects with >0.2 mm mean RMS displacement, denoising rs-

fMRI for motion-related artifacts with ICA-AROMA, employing wavelet coherence to construct the connectivity matrices and adding RMS displacement to the regression model.

In conclusion, we showed that higher global efficiency during rest and higher FC of the DMN with other RSNs and within itself is associated with slower planning performance. We tentatively postulate that due to ceiling effects individuals with a higher integrative network state during rest are less able to reconfigure to a more integrated state during task execution, leading to slower exchange across the brain network and slower behavioral responses.

Acknowledgements

The authors want to acknowledge Dr. Niels Gerrits and Dr. Stella de Wit for carrying out the data collection.

Conflict of interest

The authors have nothing to declare.

References

Achard, S., Salvador, R., Whitcher, B., Suckling, J., & Bullmore, E. (2006). A resilient, low-frequency, small-world human brain functional network with highly connected association cortical hubs. *J Neurosci, 26*(1), 63-72. Retrieved from https://www.ncbi.nlm.nih.gov/pubmed/16399673. doi:10.1523/JNEUROSCI.3874-05.2006

Ajilore, O., Lamar, M., & Kumar, A. (2014). Association of brain network efficiency with aging, depression, and cognition. *Am J Geriatr Psychiatry, 22*(2), 102-110. Retrieved from https://www.ncbi.nlm.nih.gov/pubmed/24200596. doi:10.1016/j.jagp.2013.10.004

Anticevic, A., Cole, M. W., Murray, J. D., Corlett, P. R., Wang, X. J., & Krystal, J. H. (2012). The role of default network deactivation in cognition and disease. *Trends Cogn Sci, 16*(12), 584-592. Retrieved from https://www.ncbi.nlm.nih.gov/pubmed/23142417. doi:10.1016/j.tics.2012.10.008

Bassett, D. S., Wymbs, N. F., Porter, M. A., Mucha, P. J., Carlson, J. M., & Grafton, S. T. (2011). Dynamic reconfiguration of human brain networks during learning. *Proceedings of the National Academy of Sciences of the United States of America, 108*(18), 7641-7646. Retrieved from https://www.ncbi.nlm.nih.gov/pubmed/21502525. doi:10.1073/pnas.1018985108

Bassett, D. S., Wymbs, N. F., Rombach, M. P., Porter, M. A., Mucha, P. J., & Grafton, S. T. (2013). Task-based core-periphery organization of human brain dynamics. *PLoS Comput Biol, 9*(9), e1003171. doi:10.1371/journal.pcbi.1003171

Benjamini, Y., & Hochberg, Y. (1995). Controlling the False Discovery Rate - a Practical and Powerful Approach to Multiple Testing. *Journal of the Royal Statistical Society Series B-Statistical Methodology, 57*(1), 289-300. Retrieved from <Go to ISI>://WOS:A1995QE45300017.

Braun, U., Schafer, A., Walter, H., Erk, S., Romanczuk-Seiferth, N., Haddad, L., . . . Bassett, D. S. (2015). Dynamic reconfiguration of frontal brain networks during executive cognition in humans. *Proceedings of the National Academy of Sciences of the United States of America, 112*(37), 11678-11683. Retrieved from https://www.ncbi.nlm.nih.gov/pubmed/26324898. doi:10.1073/pnas.1422487112

Buckner, R. L., Andrews-Hanna, J. R., & Schacter, D. L. (2008). The brain's default network: anatomy, function, and relevance to disease. *Annals of the New York Academy of Sciences, 1124*, 1-38. Retrieved from https://www.ncbi.nlm.nih.gov/pubmed/18400922. doi:10.1196/annals.1440.011

Bullmore, E., & Sporns, O. (2009). Complex brain networks: graph theoretical analysis of structural and functional systems. *Nat Rev Neurosci, 10*(3), 186-198. Retrieved from https://www.ncbi.nlm.nih.gov/pubmed/19190637. doi:10.1038/nrn2575

Bullmore, E., & Sporns, O. (2012). The economy of brain network organization. *Nat Rev Neurosci, 13*(5), 336-349. Retrieved from https://www.ncbi.nlm.nih.gov/pubmed/22498897. doi:10.1038/nrn3214

Campbell, K. L., & Schacter, D. L. (2017). Aging and the Resting State: Is Cognition Obsolete? *Lang Cogn Neurosci, 32*(6), 661-668. Retrieved from https://www.ncbi.nlm.nih.gov/pubmed/28626776. doi:10.1080/23273798.2016.1227858

Chang, C., & Glover, G. H. (2010). Time-frequency dynamics of resting-state brain connectivity measured with fMRI. *Neuroimage, 50*(1), 81-98. Retrieved from https://www.ncbi.nlm.nih.gov/pubmed/20006716. doi:10.1016/j.neuroimage.2009.12.011

Ciric, R., Wolf, D. H., Power, J. D., Roalf, D. R., Baum, G. L., Ruparel, K., . . . Satterthwaite, T. D. (2017). Benchmarking of participant-level confound regression strategies for the control of motion artifact in studies of functional connectivity. *Neuroimage, 154*, 174-187. Retrieved from https://www.ncbi.nlm.nih.gov/pubmed/28302591. doi:10.1016/j.neuroimage.2017.03.020

Cohen, J. R., & D'Esposito, M. (2016). The Segregation and Integration of Distinct Brain Networks and Their Relationship to Cognition. *J Neurosci, 36*(48), 12083-12094. Retrieved from https://www.ncbi.nlm.nih.gov/pubmed/27903719. doi:10.1523/JNEUROSCI.2965-15.2016

Cole, D. M., Smith, S. M., & Beckmann, C. F. (2010). Advances and pitfalls in the analysis and interpretation of resting-state FMRI data. *Front Syst Neurosci, 4*, 8. Retrieved from https://www.ncbi.nlm.nih.gov/pubmed/20407579. doi:10.3389/fnsys.2010.00008

Cole, M. W., Bassett, D. S., Power, J. D., Braver, T. S., & Petersen, S. E. (2014). Intrinsic and task-evoked network architectures of the human brain. *Neuron, 83*(1), 238-251. Retrieved from https://www.ncbi.nlm.nih.gov/pubmed/24991964. doi:10.1016/j.neuron.2014.05.014

Cole, M. W., Repovs, G., & Anticevic, A. (2014). The frontoparietal control system: a central role in mental health. *Neuroscientist, 20*(6), 652-664. Retrieved from https://www.ncbi.nlm.nih.gov/pubmed/24622818. doi:10.1177/1073858414525995

Cole, M. W., Yarkoni, T., Repovs, G., Anticevic, A., & Braver, T. S. (2012). Global connectivity of prefrontal cortex predicts cognitive control and intelligence. *J Neurosci, 32*(26), 8988-8999. Retrieved from https://www.ncbi.nlm.nih.gov/pubmed/22745498. doi:10.1523/JNEUROSCI.0536-12.2012

Dai, Z., Lin, Q., Li, T., Wang, X., Yuan, H., Yu, X., . . . Wang, H. (2019). Disrupted structural and functional brain networks in Alzheimer's disease. *Neurobiol Aging, 75*, 71-82. Retrieved from https://www.ncbi.nlm.nih.gov/pubmed/30553155. doi:10.1016/j.neurobiolaging.2018.11.005

Davis, S. W., Stanley, M. L., Moscovitch, M., & Cabeza, R. (2017). Resting-state networks do not determine cognitive function networks: a commentary on Campbell and Schacter (2016). *Lang Cogn Neurosci, 32*(6), 669-673. Retrieved from https://www.ncbi.nlm.nih.gov/pubmed/28989941. doi:10.1080/23273798.2016.1252847

Davison, E. N., Schlesinger, K. J., Bassett, D. S., Lynall, M. E., Miller, M. B., Grafton, S. T., & Carlson, J. M. (2015). Brain network adaptability across task states. *PLoS Computational Biology, 11*(1), e1004029. Retrieved from https://www.ncbi.nlm.nih.gov/pubmed/25569227. doi:10.1371/journal.pcbi.1004029

de Wit, S. J., de Vries, F. E., van der Werf, Y. D., Cath, D. C., Heslenfeld, D. J., Veltman, E. M., . . . van den Heuvel, O. A. (2012). Presupplementary motor area hyperactivity during response inhibition: a candidate endophenotype of obsessive-compulsive disorder. *American Journal of Psychiatry, 169*(10), 1100-1108. Retrieved from https://www.ncbi.nlm.nih.gov/pubmed/23032388. doi:10.1176/appi.ajp.2012.12010073

Diamond, A. (2013). Executive functions. *Annual Review of Psychology, 64*, 135-168. Retrieved from https://www.ncbi.nlm.nih.gov/pubmed/23020641. doi:10.1146/annurev-psych-113011-143750

Diedrichsen, J., Balsters, J. H., Flavell, J., Cussans, E., & Ramnani, N. (2009). A probabilistic MR atlas of the human cerebellum. *Neuroimage, 46*(1), 39-46. Retrieved from https://www.ncbi.nlm.nih.gov/pubmed/19457380. doi:10.1016/j.neuroimage.2009.01.045

Esposito, R., Cieri, F., Chiacchiaretta, P., Cera, N., Lauriola, M., Di Giannantonio, M., . . . Ferretti, A. (2018). Modifications in resting state functional anticorrelation between default mode network and dorsal attention network: comparison among young adults, healthy elders and mild cognitive impairment patients. *Brain Imaging Behav, 12*(1), 127-141. Retrieved from https://www.ncbi.nlm.nih.gov/pubmed/28176262. doi:10.1007/s11682-017-9686-y

Fadili, M. J., & Bullmore, E. T. (2004). A comparative evaluation of wavelet-based methods for hypothesis testing of brain activation maps. *Neuroimage, 23*(3), 1112-1128. Retrieved from https://www.ncbi.nlm.nih.gov/pubmed/15528111. doi:10.1016/j.neuroimage.2004.07.034

Fan, L., Li, H., Zhuo, J., Zhang, Y., Wang, J., Chen, L., . . . Jiang, T. (2016). The Human Brainnetome Atlas: A New Brain Atlas Based on Connectional Architecture. *Cerebral Cortex, 26*(8), 3508-3526. Retrieved from https://www.ncbi.nlm.nih.gov/pubmed/27230218. doi:10.1093/cercor/bhw157

Fortenbaugh, F. C., Rothlein, D., McGlinchey, R., DeGutis, J., & Esterman, M. (2018). Tracking behavioral and neural fluctuations during sustained attention: A robust replication and extension. *Neuroimage, 171*, 148-164. Retrieved from https://www.ncbi.nlm.nih.gov/pubmed/29307606. doi:10.1016/j.neuroimage.2018.01.002

Funahashi, S., & Andreau, J. M. (2013). Prefrontal cortex and neural mechanisms of executive function. *Journal of Physiology, Paris, 107*(6), 471-482. Retrieved from https://www.ncbi.nlm.nih.gov/pubmed/23684970. doi:10.1016/j.jphysparis.2013.05.001

Gerrits, N. J., van der Werf, Y. D., Verhoef, K. M., Veltman, D. J., Groenewegen, H. J., Berendse, H. W., & van den Heuvel, O. A. (2015). Compensatory fronto-parietal hyperactivation during set-shifting in unmedicated patients with Parkinson's disease. *Neuropsychologia, 68*, 107-116. Retrieved from https://www.ncbi.nlm.nih.gov/pubmed/25576907. doi:10.1016/j.neuropsychologia.2014.12.022

Gratton, C., Laumann, T. O., Nielsen, A. N., Greene, D. J., Gordon, E. M., Gilmore, A. W., . . . Petersen, S. E. (2018). Functional Brain Networks Are Dominated by Stable Group and Individual Factors, Not Cognitive or Daily Variation. *Neuron, 98*(2), 439-452 e435. Retrieved from https://www.ncbi.nlm.nih.gov/pubmed/29673485. doi:10.1016/j.neuron.2018.03.035

Griffa, A., Baumann, P. S., Thiran, J. P., & Hagmann, P. (2013). Structural connectomics in brain diseases. *Neuroimage, 80*, 515-526. Retrieved from http://www.ncbi.nlm.nih.gov/pubmed/23623973. doi:10.1016/j.neuroimage.2013.04.056

Gu, S., Yang, M., Medaglia, J. D., Gur, R. C., Gur, R. E., Satterthwaite, T. D., & Bassett, D. S. (2017). Functional hypergraph uncovers novel covariant structures over neurodevelopment. *Hum Brain Mapp, 38*(8), 3823-3835. Retrieved from https://www.ncbi.nlm.nih.gov/pubmed/28493536. doi:10.1002/hbm.23631

Hearne, L. J., Cocchi, L., Zalesky, A., & Mattingley, J. B. (2017). Reconfiguration of Brain Network Architectures between Resting-State and Complexity-Dependent Cognitive Reasoning. *J Neurosci, 37*(35), 8399-8411. Retrieved from https://www.ncbi.nlm.nih.gov/pubmed/28760864. doi:10.1523/JNEUROSCI.0485-17.2017

Iordan, A. D., & Reuter-Lorenz, P. A. (2017). Age-related change and the predictive value of the "Resting state": a commentary on Campbell and Schacter (2016). *Language, Cognition and Neuroscience, 32*(6), 674-677. Retrieved from https://doi.org/10.1080/23273798.2016.1242759. doi:10.1080/23273798.2016.1242759

Ito, T., Kulkarni, K. R., Schultz, D. H., Mill, R. D., Chen, R. H., Solomyak, L. I., & Cole, M. W. (2017). Cognitive task information is transferred between brain regions via resting-state network topology. *Nature Communications, 8*(1), 1027. Retrieved from https://doi.org/10.1038/s41467-017-01000-w. doi:10.1038/s41467-017-01000-w

Kaller, C. P., Debelak, R., Kostering, L., Egle, J., Rahm, B., Wild, P. S., . . . Unterrainer, J. M. (2016). Assessing Planning Ability Across the Adult Life Span: Population-Representative and Age-Adjusted Reliability Estimates for the Tower of London (TOL-F). *Archives of Clinical Neuropsychology, 31*(2), 148-164. Retrieved from https://www.ncbi.nlm.nih.gov/pubmed/26715472. doi:10.1093/arclin/acv088

Krienen, F. M., Yeo, B. T., & Buckner, R. L. (2014). Reconfigurable task-dependent functional coupling modes cluster around a core functional architecture. *Philos Trans R Soc Lond B Biol Sci, 369*(1653). Retrieved from https://www.ncbi.nlm.nih.gov/pubmed/25180304. doi:10.1098/rstb.2013.0526

Langer, N., Pedroni, A., Gianotti, L. R., Hanggi, J., Knoch, D., & Jancke, L. (2012). Functional brain network efficiency predicts intelligence. *Hum Brain Mapp, 33*(6), 1393-1406. Retrieved from https://www.ncbi.nlm.nih.gov/pubmed/21557387. doi:10.1002/hbm.21297

Latora, V., & Marchiori, M. (2001). Efficient behavior of small-world networks. *Physical Review Letters, 87*(19), 198701. Retrieved from https://www.ncbi.nlm.nih.gov/pubmed/11690461. doi:10.1103/PhysRevLett.87.198701

Lopes, R., Delmaire, C., Defebvre, L., Moonen, A. J., Duits, A. A., Hofman, P., . . . Dujardin, K. (2017). Cognitive phenotypes in parkinson's disease differ in terms of brain-network organization and connectivity. *Hum Brain Mapp, 38*(3), 1604-1621. Retrieved from https://www.ncbi.nlm.nih.gov/pubmed/27859960. doi:10.1002/hbm.23474

Lord, L. D., Stevner, A. B., Deco, G., & Kringelbach, M. L. (2017). Understanding principles of integration and segregation using whole-brain computational connectomics: implications for

neuropsychiatric disorders. *Philos Trans A Math Phys Eng Sci, 375*(2096). Retrieved from https://www.ncbi.nlm.nih.gov/pubmed/28507228. doi:10.1098/rsta.2016.0283

Mak, L. E., Minuzzi, L., MacQueen, G., Hall, G., Kennedy, S. H., & Milev, R. (2017). The Default Mode Network in Healthy Individuals: A Systematic Review and Meta-Analysis. *Brain Connect, 7*(1), 25-33. Retrieved from https://www.ncbi.nlm.nih.gov/pubmed/27917679. doi:10.1089/brain.2016.0438

Meijer, K. A., Eijlers, A. J. C., Douw, L., Uitdehaag, B. M. J., Barkhof, F., Geurts, J. J. G., & Schoonheim, M. M. (2017). Increased connectivity of hub networks and cognitive impairment in multiple sclerosis. *Neurology, 88*(22), 2107-2114. Retrieved from https://www.ncbi.nlm.nih.gov/pubmed/28468841. doi:10.1212/WNL.0000000000003982

Nowrangi, M. A., Lyketsos, C., Rao, V., & Munro, C. A. (2014). Systematic review of neuroimaging correlates of executive functioning: converging evidence from different clinical populations. *Journal of Neuropsychiatry and Clinical Neurosciences, 26*(2), 114-125. Retrieved from https://www.ncbi.nlm.nih.gov/pubmed/24763759. doi:10.1176/appi.neuropsych.12070176

Oldfield, R. C. (1971). The assessment and analysis of handedness: the Edinburgh inventory. *Neuropsychologia, 9*(1), 97-113. Retrieved from https://www.ncbi.nlm.nih.gov/pubmed/5146491.

Owen, A. M. (1997). Cognitive planning in humans: neuropsychological, neuroanatomical and neuropharmacological perspectives. *Progress in Neurobiology, 53*(4), 431-450. Retrieved from https://www.ncbi.nlm.nih.gov/pubmed/9421831.

Parkes, L., Fulcher, B., Yucel, M., & Fornito, A. (2018). An evaluation of the efficacy, reliability, and sensitivity of motion correction strategies for resting-state functional MRI. *Neuroimage, 171*, 415-436. Retrieved from https://www.ncbi.nlm.nih.gov/pubmed/29278773. doi:10.1016/j.neuroimage.2017.12.073

Patenaude, B., Smith, S. M., Kennedy, D. N., & Jenkinson, M. (2011). A Bayesian model of shape and appearance for subcortical brain segmentation. *Neuroimage, 56*(3), 907-922. Retrieved from https://www.ncbi.nlm.nih.gov/pubmed/21352927. doi:10.1016/j.neuroimage.2011.02.046

Phillips, L. H., Wynn, V. E., McPherson, S., & Gilhooly, K. J. (2001). Mental planning and the Tower of London task. *Quarterly Journal of Experimental Psychology. A, Human Experimental Psychology, 54*(2), 579-597. Retrieved from https://www.ncbi.nlm.nih.gov/pubmed/11394063. doi:10.1080/713755977

Power, J. D., Schlaggar, B. L., & Petersen, S. E. (2015). Recent progress and outstanding issues in motion correction in resting state fMRI. *Neuroimage, 105*, 536-551. Retrieved from https://www.ncbi.nlm.nih.gov/pubmed/25462692. doi:10.1016/j.neuroimage.2014.10.044

Pruim, R. H. R., Mennes, M., van Rooij, D., Llera, A., Buitelaar, J. K., & Beckmann, C. F. (2015). ICA-AROMA: A robust ICA-based strategy for removing motion artifacts from fMRI data. *Neuroimage, 112*, 267-277. Retrieved from https://www.ncbi.nlm.nih.gov/pubmed/25770991. doi:10.1016/j.neuroimage.2015.02.064

Putcha, D., Ross, R. S., Cronin-Golomb, A., Janes, A. C., & Stern, C. E. (2016). Salience and Default Mode Network Coupling Predicts Cognition in Aging and Parkinson's Disease. *J Int Neuropsychol Soc, 22*(2), 205-215. Retrieved from https://www.ncbi.nlm.nih.gov/pubmed/26888617. doi:10.1017/S1355617715000892

Rabinovici, G. D., Stephens, M. L., & Possin, K. L. (2015). Executive dysfunction. *Continuum (Minneap Minn), 21*(3 Behavioral Neurology and Neuropsychiatry), 646-659. Retrieved from https://www.ncbi.nlm.nih.gov/pubmed/26039846. doi:10.1212/01.CON.0000466658.05156.54

Rocca, M. A., Valsasina, P., Meani, A., Falini, A., Comi, G., & Filippi, M. (2016). Impaired functional integration in multiple sclerosis: a graph theory study. *Brain Struct Funct, 221*(1), 115-131. Retrieved from https://www.ncbi.nlm.nih.gov/pubmed/25257603. doi:10.1007/s00429-014-0896-4

Rubinov, M., & Sporns, O. (2010). Complex network measures of brain connectivity: uses and interpretations. *Neuroimage, 52*(3), 1059-1069. Retrieved from https://www.ncbi.nlm.nih.gov/pubmed/19819337. doi:10.1016/j.neuroimage.2009.10.003

Schmand, B. A., Bakker, D., Saan, R. J., & Louman, J. (1991). De Nederlandse Leestest voor Volwassenen: een maat voor het premorbide intelligentieniveau. *Tijdschrift voor Gerontologie en Geriatrie %@ 0167-9228*.

Shallice, T. (1982). Specific impairments of planning. *Philos Trans R Soc Lond B Biol Sci, 298*(1089), 199-209. Retrieved from https://www.ncbi.nlm.nih.gov/pubmed/6125971. doi:10.1098/rstb.1982.0082

Sheffield, J. M., Kandala, S., Tamminga, C. A., Pearlson, G. D., Keshavan, M. S., Sweeney, J. A., . . . Barch, D. M. (2017). Transdiagnostic Associations Between Functional Brain Network Integrity and Cognition. *JAMA Psychiatry, 74*(6), 605-613. Retrieved from https://www.ncbi.nlm.nih.gov/pubmed/28467520. doi:10.1001/jamapsychiatry.2017.0669

Sheffield, J. M., Repovs, G., Harms, M. P., Carter, C. S., Gold, J. M., MacDonald, A. W., 3rd, . . . Barch, D. M. (2015). Fronto-parietal and cingulo-opercular network integrity and cognition in health and schizophrenia. *Neuropsychologia, 73*, 82-93. Retrieved from https://www.ncbi.nlm.nih.gov/pubmed/25979608. doi:10.1016/j.neuropsychologia.2015.05.006

Shine, J. M., Bissett, P. G., Bell, P. T., Koyejo, O., Balsters, J. H., Gorgolewski, K. J., . . . Poldrack, R. A. (2016). The Dynamics of Functional Brain Networks: Integrated Network States during Cognitive Task Performance. *Neuron, 92*(2), 544-554. Retrieved from https://www.ncbi.nlm.nih.gov/pubmed/27693256. doi:10.1016/j.neuron.2016.09.018

Shine, J. M., & Poldrack, R. A. (2018). Principles of dynamic network reconfiguration across diverse brain states. *Neuroimage, 180*(Pt B), 396-405. Retrieved from https://www.ncbi.nlm.nih.gov/pubmed/28782684. doi:10.1016/j.neuroimage.2017.08.010

Smith, S. M., Jenkinson, M., Woolrich, M. W., Beckmann, C. F., Behrens, T. E., Johansen-Berg, H., . . . Matthews, P. M. (2004). Advances in functional and structural MR image analysis and implementation as FSL. *Neuroimage, 23 Suppl 1*, S208-219. Retrieved from https://www.ncbi.nlm.nih.gov/pubmed/15501092. doi:10.1016/j.neuroimage.2004.07.051

Stanley, M. L., Simpson, S. L., Dagenbach, D., Lyday, R. G., Burdette, J. H., & Laurienti, P. J. (2015). Changes in brain network efficiency and working memory performance in aging. *PLoS One, 10*(4), e0123950. Retrieved from https://www.ncbi.nlm.nih.gov/pubmed/25875001. doi:10.1371/journal.pone.0123950

Telesford, Q. K., Lynall, M. E., Vettel, J., Miller, M. B., Grafton, S. T., & Bassett, D. S. (2016). Detection of functional brain network reconfiguration during task-driven cognitive states. *Neuroimage, 142*, 198-210. Retrieved from http://www.ncbi.nlm.nih.gov/pubmed/27261162. doi:10.1016/j.neuroimage.2016.05.078

van den Heuvel, M. P., Stam, C. J., Kahn, R. S., & Hulshoff Pol, H. E. (2009). Efficiency of functional brain networks and intellectual performance. *J Neurosci, 29*(23), 7619-7624. Retrieved from https://www.ncbi.nlm.nih.gov/pubmed/19515930. doi:10.1523/JNEUROSCI.1443-09.2009

van den Heuvel, O. A., Groenewegen, H. J., Barkhof, F., Lazeron, R. H., van Dyck, R., & Veltman, D. J. (2003). Frontostriatal system in planning complexity: a parametric functional magnetic resonance version of Tower of London task. *Neuroimage, 18*(2), 367-374. Retrieved from https://www.ncbi.nlm.nih.gov/pubmed/12595190.

Verhage, F. (1964). *Intelligentie en leeftijd: Onderzoek bij Nederlands van twaal tot zevenenzeventig jaar.* . Assen, the Netherlands: van Gorcum.

Wang, J., Zuo, X., & He, Y. (2010). Graph-based network analysis of resting-state functional MRI. *Front Syst Neurosci, 4*, 16. Retrieved from https://www.ncbi.nlm.nih.gov/pubmed/20589099. doi:10.3389/fnsys.2010.00016

Worbe, Y. (2015). Neuroimaging signature of neuropsychiatric disorders. *Curr Opin Neurol, 28*(4), 358-364. Retrieved from http://www.ncbi.nlm.nih.gov/pubmed/26110796. doi:10.1097/WCO.0000000000000220

Yeo, B. T., Krienen, F. M., Sepulcre, J., Sabuncu, M. R., Lashkari, D., Hollinshead, M., . . . Buckner, R. L. (2011). The organization of the human cerebral cortex estimated by intrinsic functional connectivity. *Journal of Neurophysiology, 106*(3), 1125-1165. Retrieved from https://www.ncbi.nlm.nih.gov/pubmed/21653723. doi:10.1152/jn.00338.2011

Zhang, Z., Telesford, Q. K., Giusti, C., Lim, K. O., & Bassett, D. S. (2016). Choosing Wavelet Methods, Filters, and Lengths for Functional Brain Network Construction. *PLoS One, 11*(6), e0157243. Retrieved from https://www.ncbi.nlm.nih.gov/pubmed/27355202. doi:10.1371/journal.pone.0157243

Figure legends

Figure 1. Outline of the processing pipeline. (A) Resting-state fMRI data were collected and (B) pre-processed. The brain was (C) parcellated into separate brain regions (nodes). There were 194 nodes common to all subjects with enough signal to (D) construct connectivity matrices (see text) using wavelet coherence. (E) network measures were calculated from each connectivity matrix on the global and subnetwork level. (F) multiple regression analyses were applied to relate performance on the Tower of London (ToL) task to network measures.

Figure 2. Flowchart of participant exclusion.

Figure 3. Partial correlation plot of association between reaction time on the Tower of London task and Global (whole-brain) efficiency. Abbreviations: ToL = Tower of London. RMS disp. = mean root-mean-squared framewise displacement.

Figure 4. Schematic representation of rest-to-task reconfiguration hypothesis. The figure shows three fictional subjects that transition from a resting-state to task state and show a concomitant increase in (global) efficiency. The top two subjects, already have such a high efficiency during resting-state that when the brain network needs to reconfigure to a more integrated state to meet task demands, efficiency cannot surpass the ceiling (horizontal dotted lines) and leads to slower responses.

TABLES

Table 1 – Sample characteristics

N subjects (% female)	62 (46.8)
Age (years)	48.1 ± 13.9
Education level (in %)#	
3	1.6
4	48
5	29.0
6	43.5
7	17.7
Handedness (R/L)*	54/7
ToL accuracy (%)	87.7 ± 7.5
ToL reaction time (s)	10.1 ± 2.1
Mean relative RMS	0.07 ± 0.03

missing for two subjects, * missing for one subject

Table 2 – associations between TOL performance and global network measures

TOL	Model	B (SE)	95% CI (BCa)	Beta	P_{bCa}	R^2
RT	Age	0.09 (0.015)	0.06, 0.12	.595	<.001	
	GE	9.79 (4.72)	0.84, 19.8	.219	.039	.293
	Motion	-16.46 (6.53)	-30.6, -5.7	-.230	.008	
	Age	0.08 (0.017)	0.04, 0.11	.531	<.001	
	Gcc	-32.88 (53.72)	-133.9, 68.8	-.089	.567	.252
	Motion	-12.03 (7.69)	-26.6, 2.3	-.168	.113	
ACC	Age	-0.131 (.073)	-0.28, -0.009	-.241	.079	
	GE	-31.1 (21.57)	-76.3, 9.6	-.194	.156	.06
	Motion	-21.62 (29.23)	-69.0, 43.1	-.084	.450	
	Age	-0.09 (.075)	-0.24, 0.05	-.164	.249	
	Gcc	206.28 (155.46)	-79.3, 515.3	.154	.187	.05
	Motion	-41.39 (27.02)	-89.5, 13.3	-.161	.117	

For each analysis, age was entered in model 1, the network measure in model 2 and motion parameters in model 3. Only the results of model 3 are shown here. P-values are bootstrapped using 2000 permutations. Abbreviations: TOL = Tower of London task, RT = reaction time, ACC = accuracy, SE = Standard Error, CI = confidence interval, BCa= Bias corrected and accelerated, GE = Global Efficiency, Gcc = Global Clustering Coefficient. Motion was defined as the mean root-mean-squared framewise displacement during the entire resting-state MRI scan.

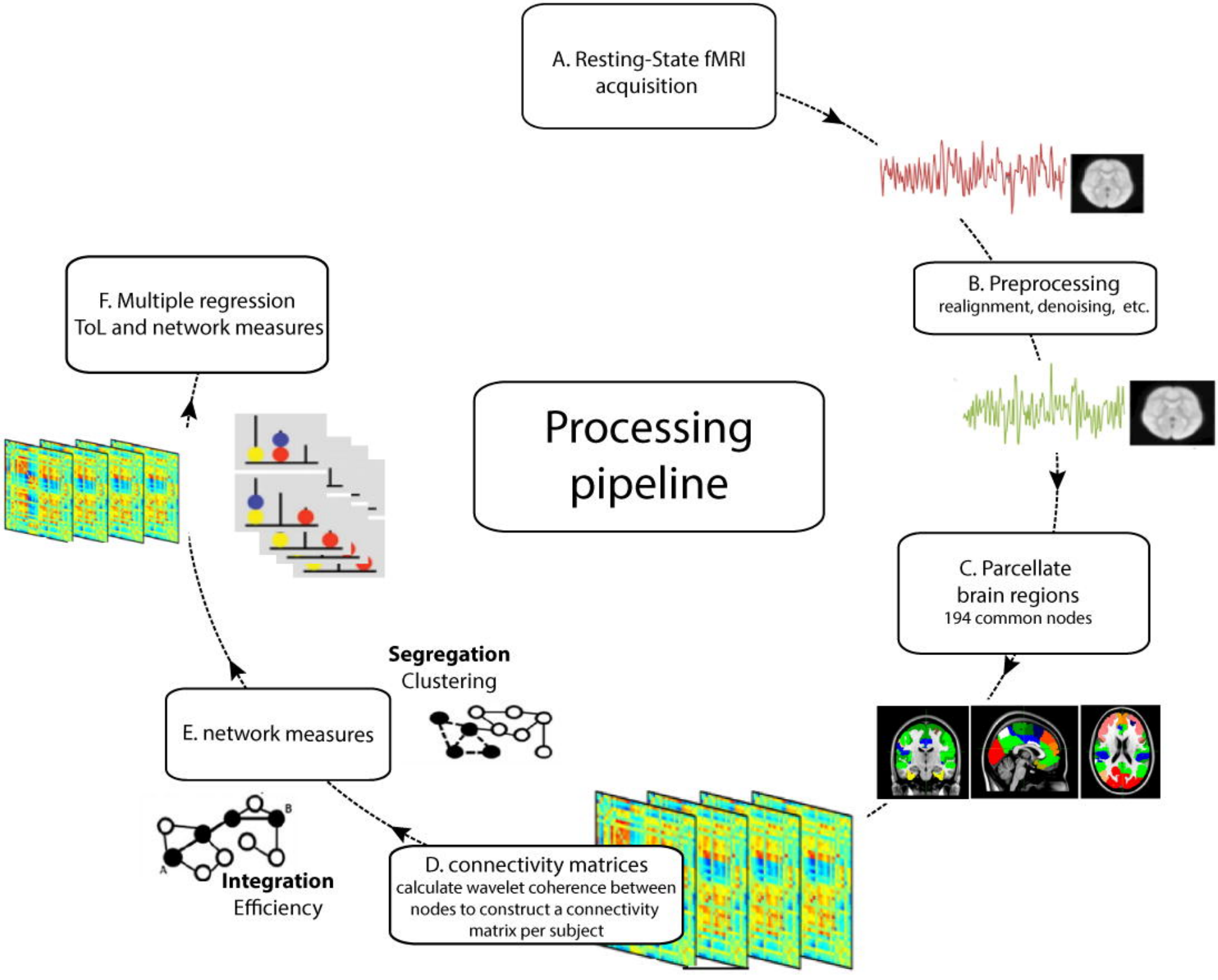
A. Resting-State fMRI acquisition
B. Preprocessing
realignment, denoising, etc.
C. Parcellate brain regions
194 common nodes
D. connectivity matrices
calculate wavelet coherence between nodes to construct a connectivity matrix per subject
E. network measures
Segregation
Clustering
Integration
Efficiency
F. Multiple regression
ToL and network measures
Processing pipeline

Flow Chart

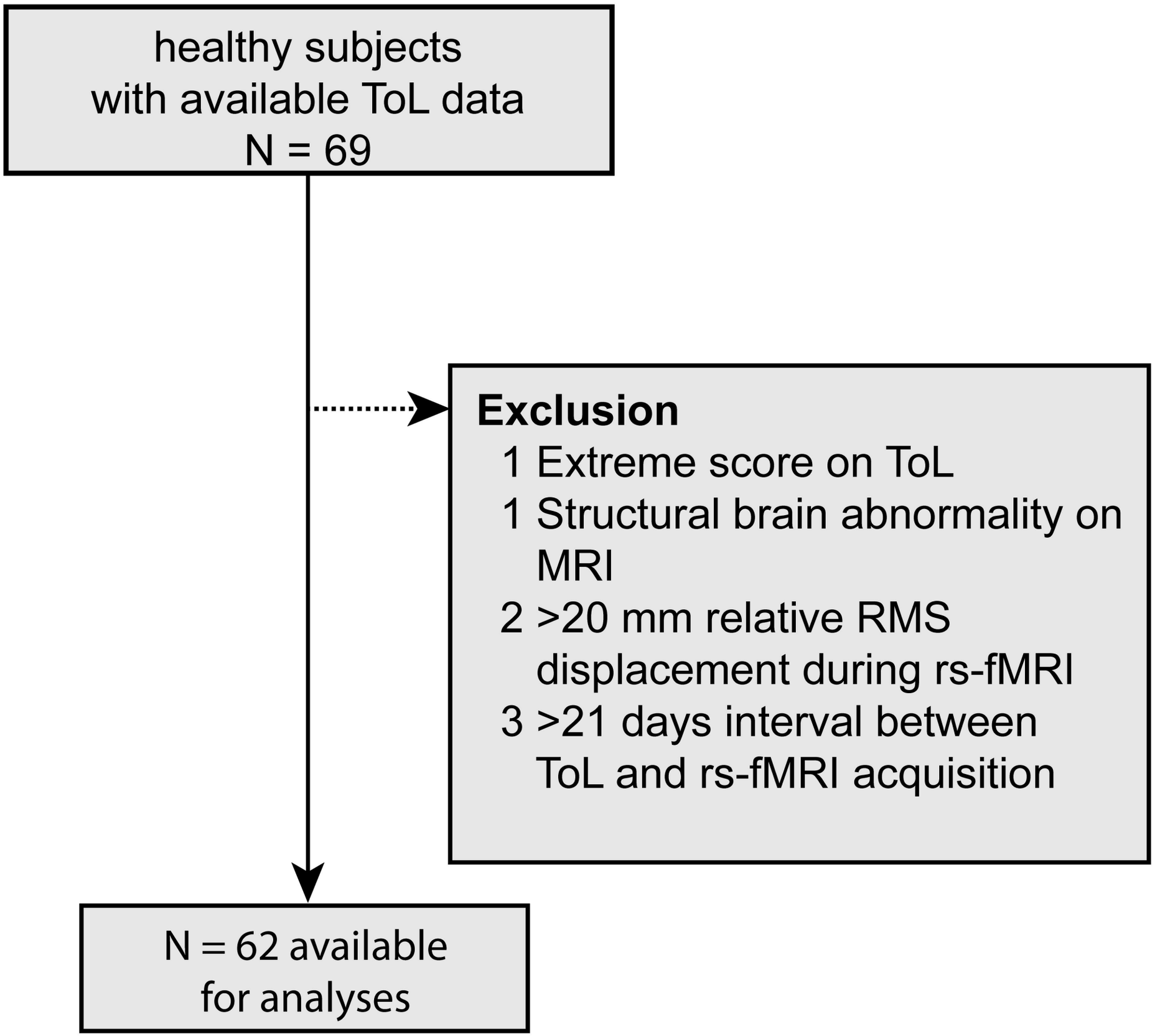
healthy subjects
with available ToL data
N = 69
Exclusion
1 Extreme score on ToL
1 Structural brain abnormality on MRI
2 >20 mm relative RMS displacement during rs-fMRI
3 >21 days interval between ToL and rs-fMRI acquisition
N = 62 available
for analyses

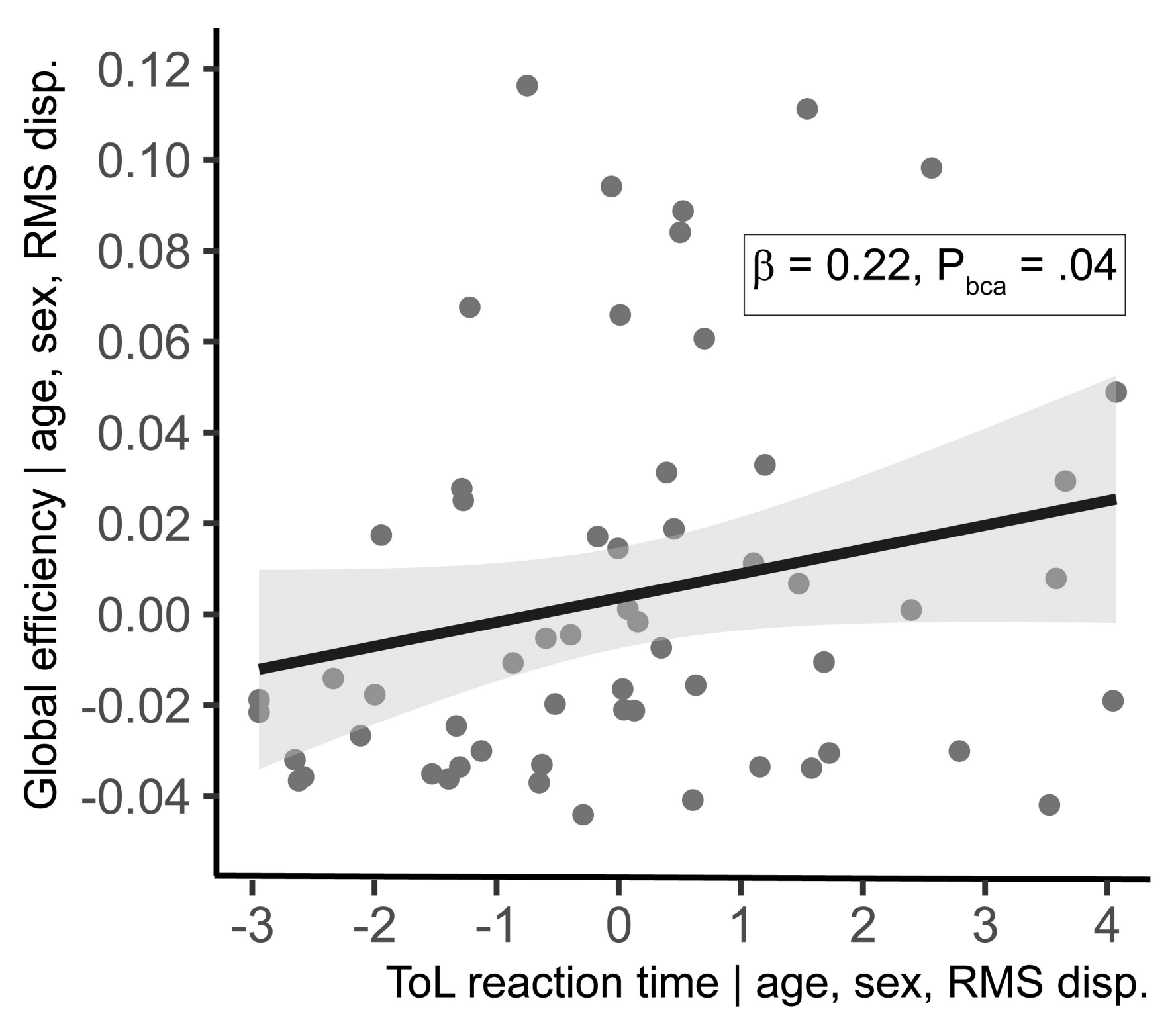
Global efficiency | age, sex, RMS disp.
0.12
0.10
0.08
0.06
0.04
0.02
0.00
-0.02
-0.04
β = 0.22, P bca = .04
-3
-2
-1
0
1
2
3
4
ToL reaction time | age, sex, RMS disp.

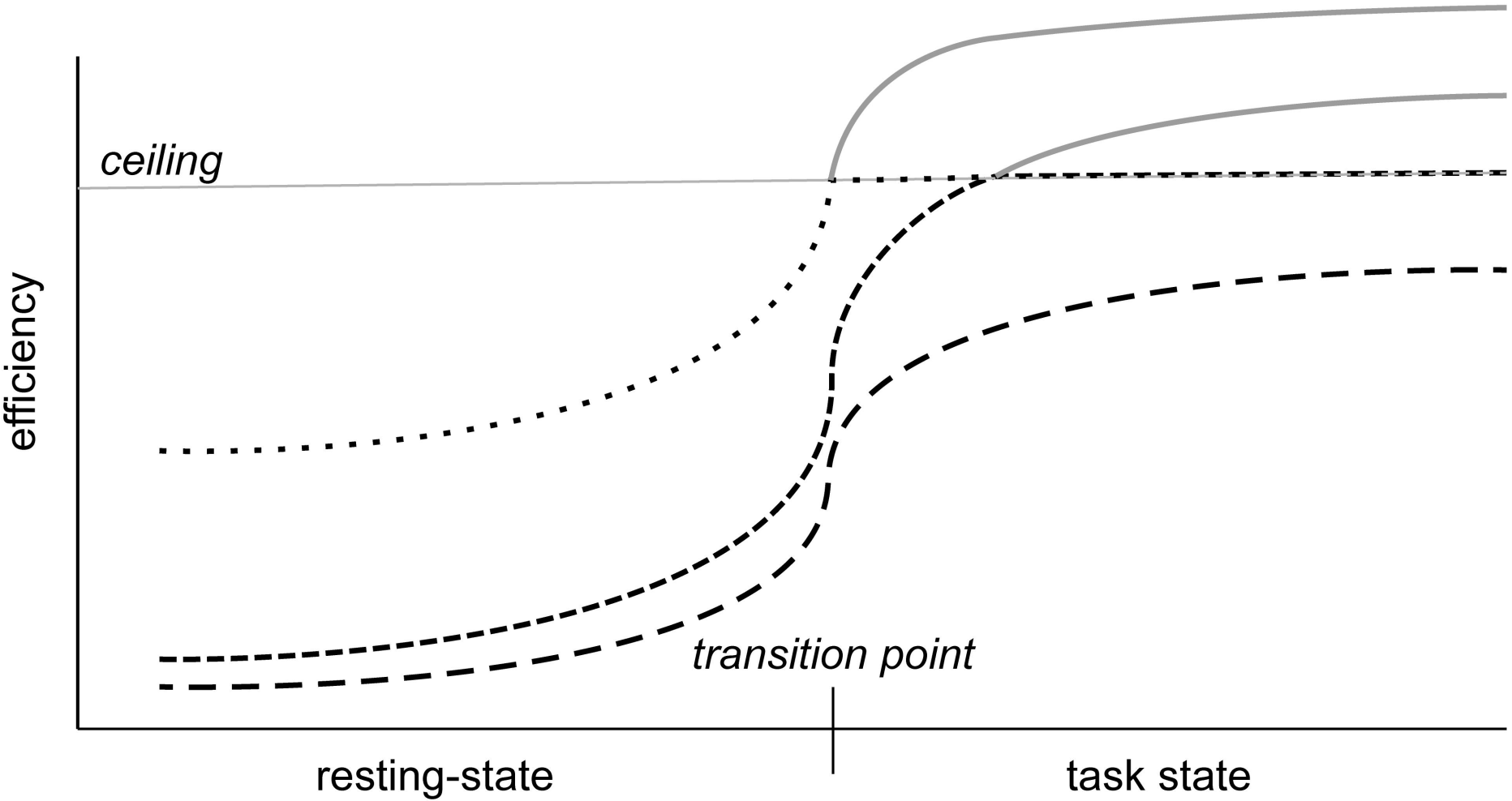
ceiling
efficiency
transition point
resting-state
task state